

Article

Ground-Based MAX-DOAS Observation of Trace Gases from 2019 to 2021 in Huaibei, China

Fusheng Mou^{1,2}, Jing Luo^{1,2}, Qijin Zhang^{1,2}, Chuang Zhou^{1,2}, Song Wang^{1,2}, Fan Ye^{1,2}, Suwen Li^{1,2} and Youwen Sun^{3,*}

¹ School of Physics and Electronic Information, Huaibei Normal University, Huaibei 235000, China; fsmou@chnu.edu.cn (F.M.); 12006110684@chnu.edu.cn (Q.Z.); 12111060763@chnu.edu.cn (C.Z.); 12211060769@chnu.edu.cn (S.W.); 12211060772@chnu.edu.cn (F.Y.); swli@chnu.edu.cn (S.L.)

² Anhui Province Key Laboratory of Pollutant Sensitive Materials and Environmental Remediation, Huaibei 235000, China

³ Laboratory of Environmental Optics and Technology, Anhui Institute of Optics and Fine Mechanics, Hefei Institutes of Physical Science, Chinese Academy of Sciences, Hefei 230031, China

* Correspondence: ywsun@aiofm.ac.cn

Abstract: With the spread of the COVID-19 pandemic and the implementation of closure measures in 2020, population mobility and human activities have decreased, which has seriously impacted atmospheric quality. Huaibei City is an important coal and chemical production base in East China, which faces increasing environmental problems. The impact of anthropogenic activities on air quality in this area was investigated by comparing the COVID-19 lockdown in 2020 with the normal situation in 2021. Tropospheric NO₂, HCHO and SO₂ column densities were observed by ground-based multiple axis differential optical absorption spectroscopy (MAX-DOAS). In situ measurements for PM_{2.5}, NO₂, SO₂ and O₃ were also taken. The observation period was divided into four phases, the pre-lockdown period, phase 1 lockdown, phase 2 lockdown and the post-lockdown period. Ground-based MAX-DOAS results showed that tropospheric NO₂, HCHO and SO₂ column densities increased by 41, 14 and 14%, respectively, during phase 1 in 2021 vs. 2020. In situ results showed that NO₂ and SO₂ increased by 59 and 11%, respectively, during phase 1 in 2021 vs. 2020, but PM_{2.5} and O₃ decreased by 15 and 17%, respectively. In the phase 2 period, due to the partial lifting of control measures, the concentration of pollutants did not significantly change. The weekly MAX-DOAS results showed that there was no obvious weekend effect of pollutants in the Huaibei area, and NO₂, HCHO and SO₂ had obvious diurnal variation characteristics. In addition, the relationship between the column densities and wind speed and direction in 2020 and 2021 was studied. The results showed that, in the absence of traffic control in 2021, elevated sources in the Eastern part of the city emitted large amounts of NO₂. The observed ratios of HCHO to NO₂ suggested that tropospheric ozone production involved NO_x-limited scenarios. The correlation analysis between HCHO and different gases showed that HCHO mainly originated from primary emission sources related to SO₂.

Keywords: MAX-DOAS; remote sensing; NO₂; SO₂; HCHO; lockdown; diurnal variation; COVID-19



Citation: Mou, F.; Luo, J.; Zhang, Q.; Zhou, C.; Wang, S.; Ye, F.; Li, S.; Sun, Y. Ground-Based MAX-DOAS Observation of Trace Gases from 2019 to 2021 in Huaibei, China. *Atmosphere* **2023**, *14*, 739. <https://doi.org/10.3390/atmos14040739>

Academic Editors: Chengzhi Xing, Yan Xiang and Qihua Li

Received: 23 February 2023

Revised: 14 April 2023

Accepted: 16 April 2023

Published: 19 April 2023



Copyright: © 2023 by the authors. Licensee MDPI, Basel, Switzerland. This article is an open access article distributed under the terms and conditions of the Creative Commons Attribution (CC BY) license (<https://creativecommons.org/licenses/by/4.0/>).

1. Introduction

Nitrogen dioxide (NO₂), formaldehyde (HCHO) and sulfur dioxide (SO₂) are important atmospheric constituents that play crucial roles in tropospheric chemistry. NO₂ is involved in the formation cycle of tropospheric ozone [1,2]. NO₂ and SO₂ can generate nitrate and sulfate particles by reacting with OH radicals. HCHO mainly comes from the oxidation of volatile organic compounds (VOCs) and industrial emissions. Primary emissions of HCHO are an important indicator of air quality in industrial areas [3,4]. HCHO has a short atmospheric lifetime and can be used to measure the local VOC content. NO₂, SO₂ and HCHO are important precursors to urban aerosols. Traffic, heating and industrial emissions significantly increase the background concentration of these gases in the urban

boundary and near ground layers [5–8]. Recent studies have found that aerosol particles in large cities in China mainly come from secondary formation reactions [2]. It is important to obtain spatiotemporal distribution data of air pollutants through long-term observations to understand their sources and atmospheric photochemical reaction processes. As China's urban traffic and industrial emissions have serious impacts on air quality, emission reduction plans were implemented to control pollution during the Shanghai World Expo (2010), the Asian-Pacific Economic Cooperation Conference in Beijing (APEC, 2014) and the G20 Summit in Hangzhou (2016) [9–11]. The air quality improved significantly during these events; however, it returned to previous levels soon after the end of these lockdown measures.

At the end of 2019, a novel coronavirus was reported in Wuhan, China, and the resulting disease was termed COVID-19. During the COVID-19 epidemic, the Chinese government enacted large-scale lockdown measures to stop the spread of the virus by reducing population mobility. The impact of city lockdowns on regional emissions and air quality has been studied in different regions of the world [12–17]. These studies show that pollutants, such as NO₂ and aerosols, in the atmosphere were significantly reduced during the lockdown period in 2020 compared to 2019, while the reduction in SO₂ was less pronounced and the concentration of O₃ increased significantly [18,19]. Multiple axis differential optical absorption spectroscopy (MAX-DOAS) has been widely used in air pollution monitoring and satellite data validation due to its simple structure and ability to simultaneously measure multiple pollutants [20–23].

Located in the Southern part of the North China Plain, Huaibei city is an important production base for coal and chemical products in East China. Huaibei is an industrial city with about 2 million inhabitants. Long-term MAX-DOAS observations in Huaibei have been important to understand the impact of traffic and industrial emissions on the urban atmosphere. In this study, we used the ground-based MAX-DOAS instrument installed in a suburban area of Huaibei to evaluate the sources of pollutants (i.e., NO₂, SO₂ and HCHO) and their relationships with lockdown measures and meteorological conditions from 1 December 2019 to 9 May 2020 and 1 December 2020 to 9 May 2021 (Figure S1). The observation period was divided into four stages: pre-lockdown (1 December to 23 January), phase 1 (24 January to 26 February), phase 2 (27 February to 31 March) and post-lockdown (1 April to 9 May). Although there was no lockdown during the observation period in 2021, the years were also divided into four similar stages for comparison. The variations of near-surface pollutants, including PM_{2.5}, NO₂, SO₂ and O₃, were also analyzed.

2. Experiments and Methods

2.1. Instruments and Observation Positions

A MAX-DOAS instrument developed by Airyx GmbH (Eppelheim, Germany) [24,25], shown in Figure 1a, is installed on the top of the Huaibei Normal University of Physics and Electronic Information Building (33.58° N, 116.48° E, 30 m above sea level; Figure 1c). Figure 1b shows a structural diagram of the MAX-DOAS system. The system comprises a telescope unit controlled by a two-dimensional stepping motor, two spectrometers (Avaspec-ULS2048L-USB2, UV: 300–405 nm, and VIS: 407–540 nm), and a controlling computer unit. The scattered sunlight is collected by the telescope installed outdoors and then transmitted to a spectrometer through an optical fiber. The spectrometer is placed in a temperature-controlled box at 20 °C to reduce the impact of ambient temperature changes on the spectrometer. The instrumental function of the spectrometer is approximated as a Gaussian function with a full width at a half maximum (FWHM) of 0.5 nm. The instrument was pointed south and automatically recorded the spectra of scattered sunlight in a sequence at eleven elevation angles (1, 2, 3, 4, 5, 6, 8, 10, 15, 30 and 90°). One elevation sequence scan took about 11 min, and the integration time was automatically adjusted based on the light intensity. The dark current correction was used in the QDOAS software retrieval process.

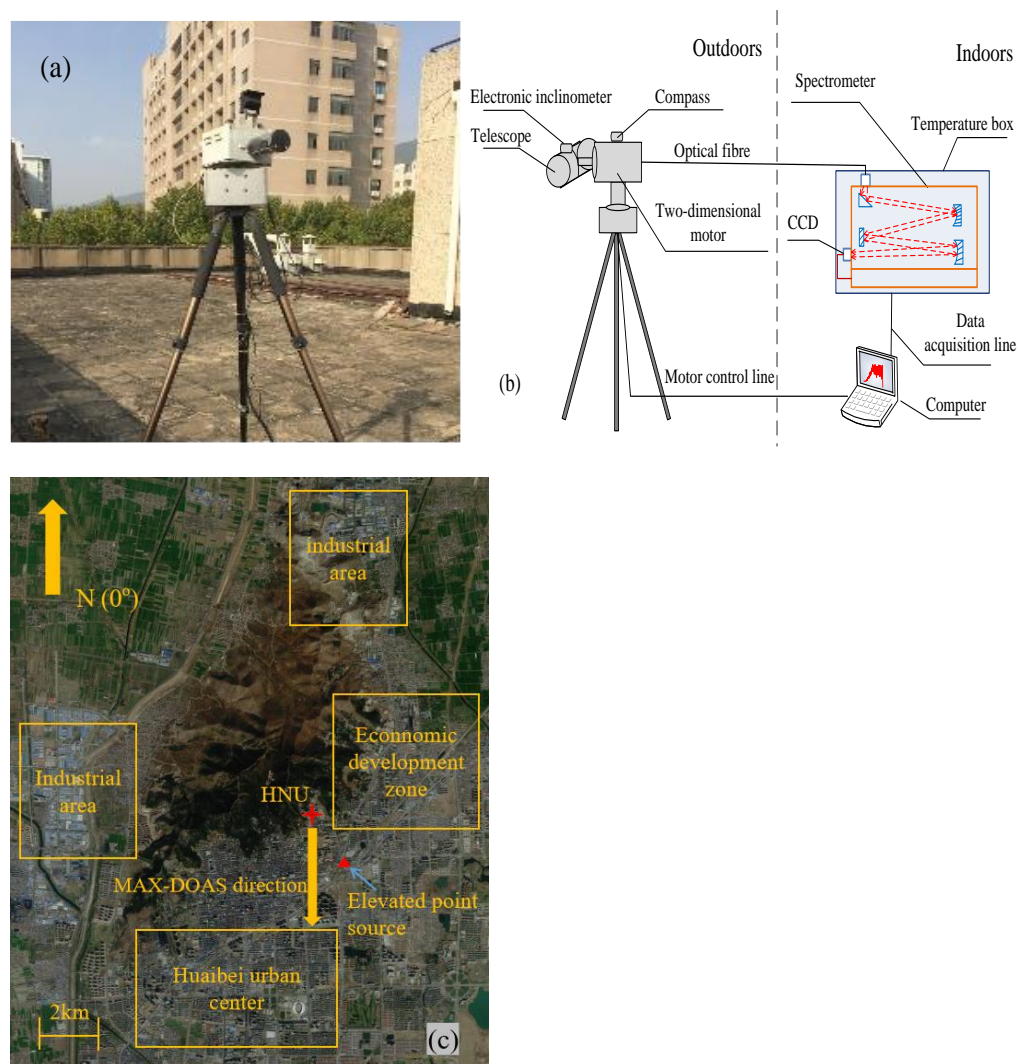


Figure 1. MAX-DOAS observation site at Huaibei Normal University. (a) Physical diagram of the system (b) Schematic diagram of the setup (c) The location of MAX-DOAS instrument at Huaibei.

2.2. Spectral Inversion and Tropospheric Column Density Measurement

The ground-based MAX-DOAS is an optical remote-sensing technology that can record scattered sunlight at different elevation angles. Trace gases can be quantitatively measured based on the Beer–Lambert law. The spectra obtained from the MAX-DOAS observations were analyzed with QDOAS software [26], and the zenith direction spectrum of the cycle was selected as the Fraunhofer reference spectrum (FRS) to calculate the differential slant column density (dSCD) and vertical column density (VCD) [27]. The trace gas cross-sections, wavelength ranges and additional properties of the DOAS analysis are provided in Table 1. The ring structure was calculated by QDOAS software through high-precision solar spectra and instrument functions. Figure 2 shows typical DOAS fit examples. In order to reduce stronger absorptions of stratospheric species and improve the signal-to-noise ratio, the spectra with solar zenith angles (SZA) larger than 75° were removed (Table S1). The spectra with large root-mean-square (RMS) values of the residuals (3×10^{-3} for NO_2 and HCHO and 5×10^{-3} for SO_2) were also removed (Figure S2). In total, 23.3, 23.2 and 25.4% of measurements were filtered by a given criterion for NO_2 , HCHO and SO_2 , respectively.

Table 1. Parameter settings used for spectral analysis using QDOAS.

Parameters	Sources	Species		
		NO ₂	HCHO	SO ₂
Fitting interval		338–370	324.6–359	307.5–330
NO ₂	294 K, [28]	x	x	x
O ₃	223 K, [29]	x	x	x
O ₃	243 K, [29]	x	x	x
O ₄	293 K, [30]	x	x	
SO ₂	293 K, [31]			x
HCHO	293 K, [31]	x	x	x
BrO	223 K, [32]	x		x
Ring	Calculated with QDOAS	x	x	x
Polynomial degree		5	5	5
Intensity offset		constant	constant	constant

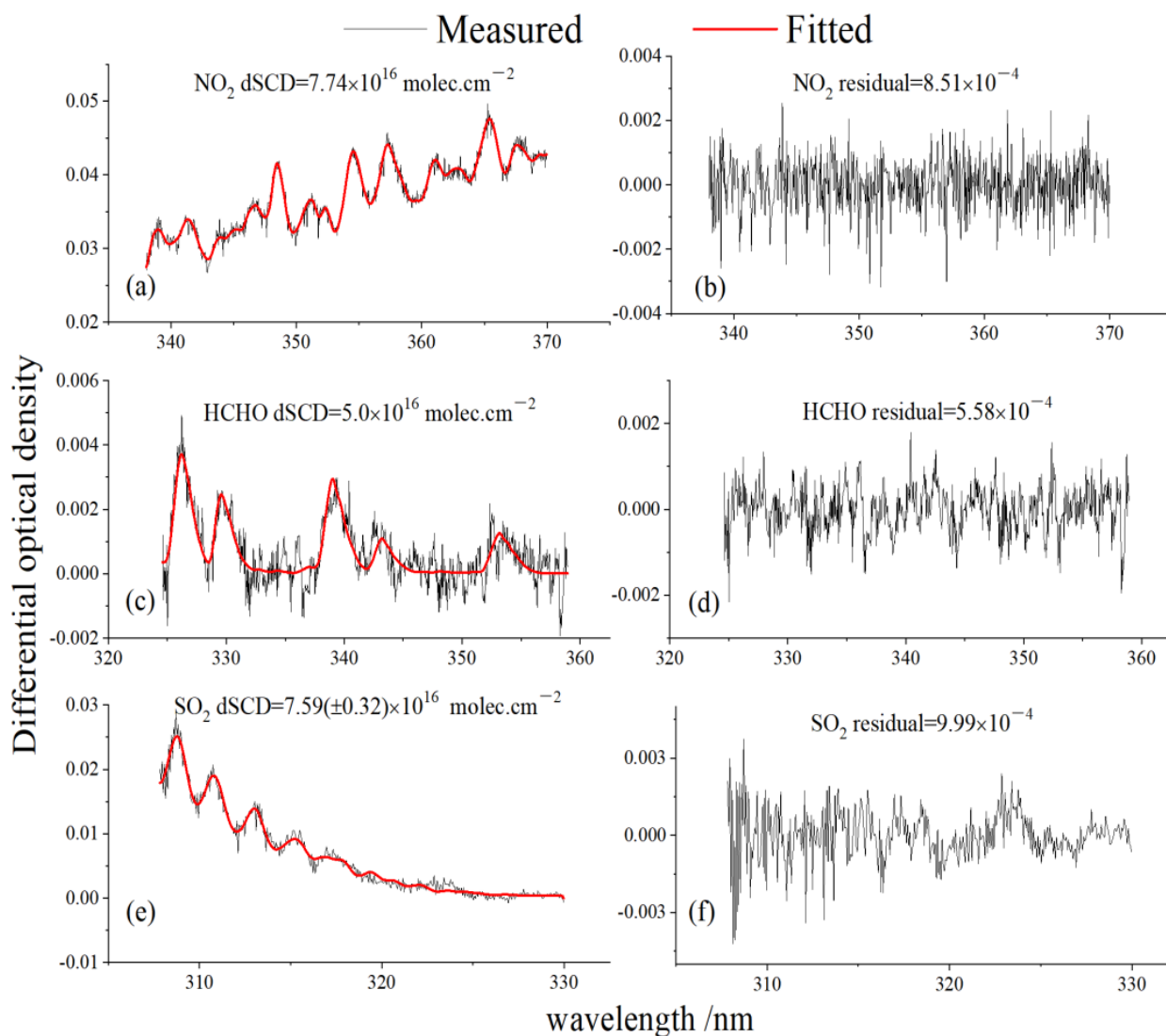


Figure 2. Examples of typical DOAS fits for NO₂ (a), HCHO (c) and SO₂ (e) at 30° elevation angle. Residuals for NO₂ (b), HCHO (d) and SO₂ (f) are given in the corresponding subfigures. The red and black curves indicate the fitted absorption structures and the derived absorption structures from the measured spectra, respectively.

The geometric approximation was used to convert the dSCDs to tropospheric VCDs [30]. The dSCDs were derived from the DOAS spectral analysis with the reference spectrum at the same observation cycle. The VCD is defined as the integrated concentration of trace gas concentrations through the atmosphere along a vertical path and is calculated from the dSCD using the differential air mass factor (dAMF) [33], as follows:

$$\text{VCD} = \frac{\text{SCD}_{\alpha \neq 90^\circ} - \text{SCD}_{\alpha = 90^\circ}}{\text{AMF}_{\alpha \neq 90^\circ} - \text{AMF}_{\alpha = 90^\circ}} = \frac{\text{dSCD}_\alpha}{\text{dAMF}_\alpha} \quad (1)$$

where α represents the elevation angle for the measurement spectrum. The AMF is used to describe the absorption path of a gas in the atmosphere.

$$\text{AMF}_\alpha = 1 / \sin \alpha \quad (2)$$

The tropospheric VCD can be obtained from the following equation:

$$\text{VCD} = \frac{\text{dSCD}_\alpha}{(1 / \sin \alpha) - 1} \quad (3)$$

This method is often used to obtain the VCD. Numerous studies have shown that the geometric light paths at 30° are good approximations (Figure S3) in the boundary layer [34,35]. The 30° and 90° elevation angles were used to calculate the VCD in this study.

2.3. Ancillary Data

The in-situ measurements for the pollutants NO_2 , SO_2 , O_3 and $\text{PM}_{2.5}$ were downloaded from <https://www.aqistudy.cn/> (last accessed on 10 April 2022). In situ data were collected using the continuous emission monitoring system (CEMS) produced by Thermo Fisher Scientific, which was installed in the urban area to monitor the near-ground air quality. The daily mean concentrations of the atmospheric pollutants were used from December 2019 to May 2021 in this study. The data of the wind speed and direction in Huaibei were downloaded from the Copernicus Data Hub (available online at <https://ads.atmosphere.copernicus.eu/>; last accessed on 15 August 2022). Near-surface temperature data were obtained from the China Meteorological Data Service Centre (CMDC, available online at <http://data.cma.cn/en>; last accessed on 16 March 2023).

3. Results

3.1. MAX-DOAS Observation Results

The observation period was from December 2019 to May 2021. The period from December 2019 to May 2020 was divided into four phases according to traffic control and compared with the corresponding period in 2021. Figure 3 shows the time-series data of the daily mean VCDs for NO_2 , HCHO and SO_2 during the observation period in 2020 and 2021. Furthermore, the observation results for NO_2 , HCHO and SO_2 showed obvious seasonal and monthly variation trends. Table 2 gives the monthly mean values during the observation period for the three gases. Since there were only nine measurement days in May, the monthly mean value for May was not calculated. The daily mean concentrations of NO_2 , HCHO and SO_2 in winter in 2020 were higher than in spring, and the daily averaged values in winter were 1.06×10^{16} molecules/cm² for NO_2 , 2.10×10^{16} molecules/cm² for HCHO, and 4.68×10^{16} molecules/cm² for SO_2 , which were 1.2, 1.8 and 2.1 times greater than those in spring, respectively. The maximum monthly mean values of the three gases occurred in December, while the minimum monthly mean values of NO_2 occurred in February and the minimum monthly mean values of HCHO and SO_2 occurred in April.

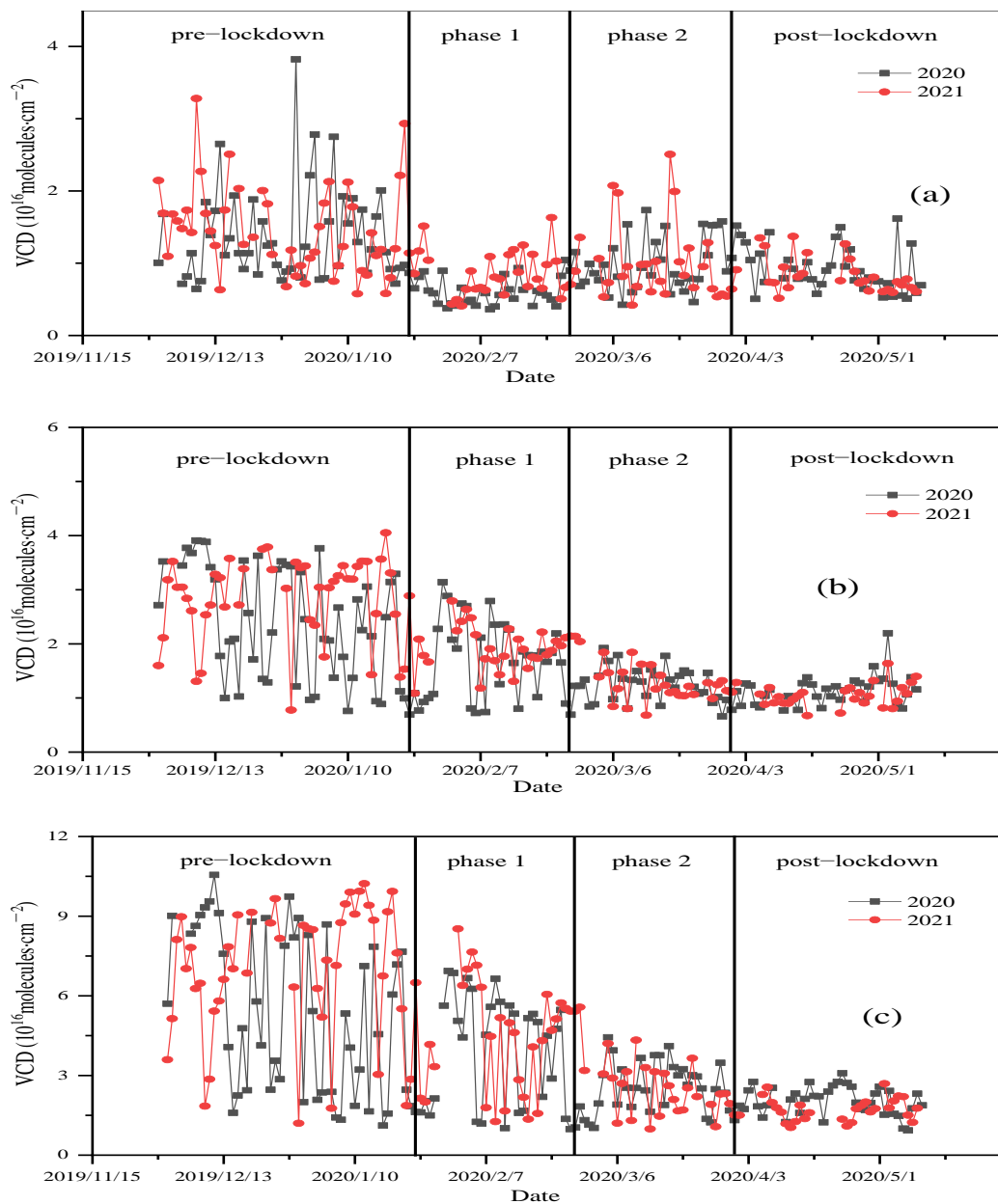


Figure 3. Time series diagram of (a) NO_2 , (b) HCHO and (c) SO_2 VCD₅ obtained by MAX-DOAS at a 30° elevation viewing angle over Huaibei. The observation period is divided into four sections.

Table 2. Monthly mean values of NO_2 , HCHO and SO_2 during the observation period (units: 10^{16} molecules/ cm^2).

		Winter			Spring	
		Mon. 12	Mon. 1	Mon. 2	Mon. 3	Mon. 4
NO_2	2019.12.1–2020.5.10	1.32	1.23	0.62	0.99	0.97
HCHO		2.79	1.85	1.67	1.24	1.10
SO_2		6.56	3.85	3.64	2.65	2.15
NO_2	2020.12.1–2021.5.10	1.57	1.29	0.84	0.98	0.91
HCHO		2.82	2.69	1.98	1.24	1.02
SO_2		6.69	6.54	4.65	2.40	1.64

In order to control the spread of COVID-19, urban traffic control measures were implemented in 2020. The MAX-DOAS observation period was divided into four stages according to the control time. There were no pandemics or traffic control measures in the Huaibei area in 2021. To study the impact of traffic control measures and the pandemic on trace gases, the results of the same period in 2020 and 2021 were compared (Table S2). Figure 4 shows the box diagram results of the three trace gases during different stages of the lockdown. In the pre-lockdown period of 2021, the concentrations of NO_2 , HCHO and SO_2 increased by 6, 20 and 32% compared to the same period in 2020. Due to the uncertainty of the epidemic and the closure measures, factories in Huaibei increased production during this period, resulting in more primary emissions. It is evident from Figure 4 that the impact of the lockdown measures on the NO_2 concentration was greater than that on the HCHO and SO_2 concentrations. Compared to the same period in 2020, the NO_2 , HCHO and SO_2 VCDs increased by 41, 14 and 14%, respectively, in phase 1 of 2021. The changes in all three gases were small during phase 2, when traffic control measures were relaxed. The main reason for this may be due to the fact that urban traffic emits a large amount of NO_2 , while SO_2 mainly comes from industrial emissions and HCHO comes from atmospheric photochemical reactions as well as industrial emissions.

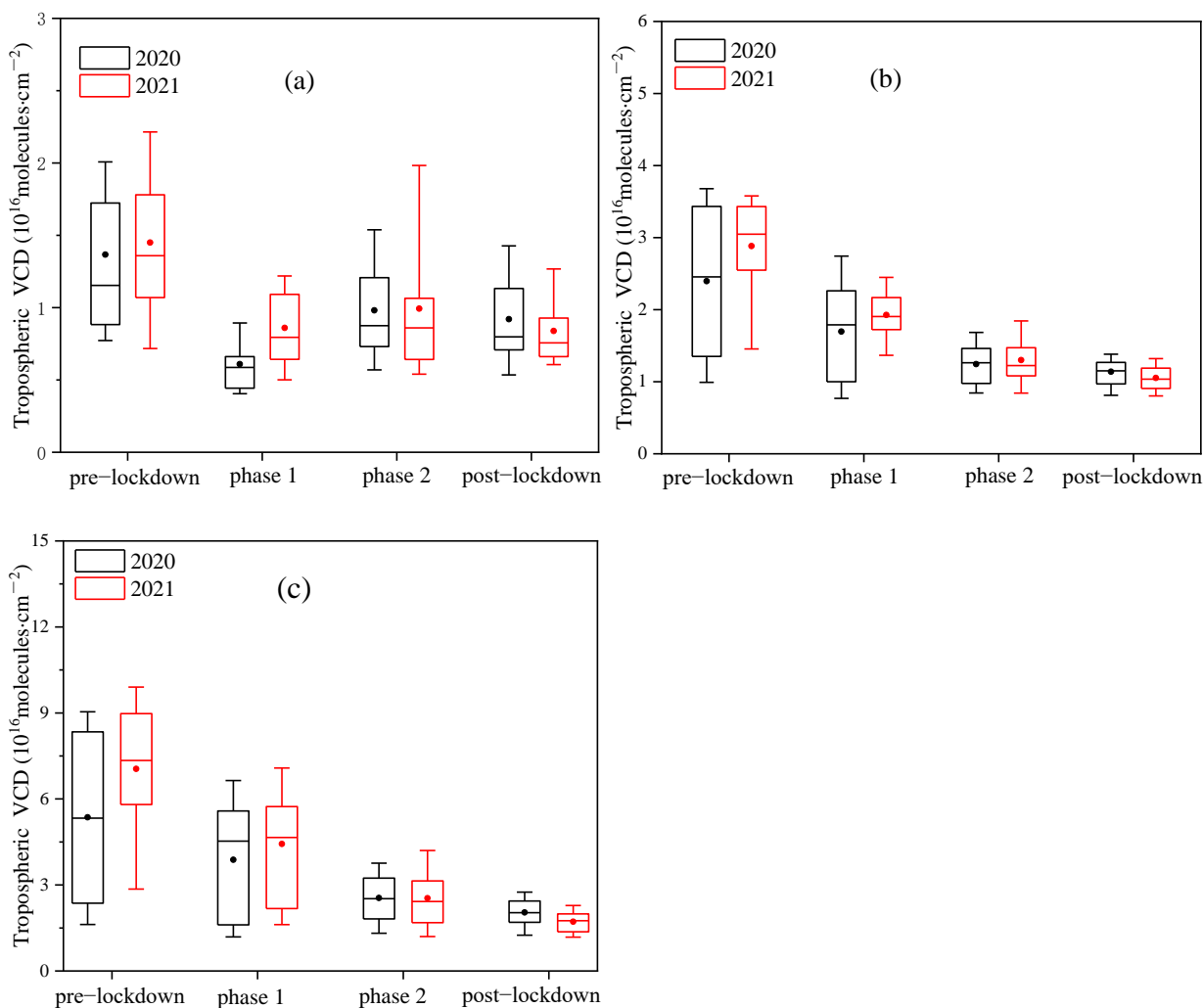


Figure 4. Box diagram of (a) NO_2 , (b) HCHO and (c) SO_2 VCD obtained by the MAX-DOAS instrument during observation. The low (upper) error bars and boxes are the 10th (90th) and 25th (75th) percentiles of the data grouped in each interval, respectively.

3.2. Weekly Circles and Diurnal Variations

To further investigate the effects of human activities on urban atmospheric trace gas concentrations, the weekly (Figure 5) and diurnal variations of the three gases were analyzed based on MAX-DOAS observations. The reduction in pollutant concentrations over the weekend due to reduced human activities is termed the weekend effect. The study period includes lockdown (phases 1 and 2) in 2020, with normal day measurements for the same period in 2021 as a comparison. The weekly concentrations of the three gases are similar in both years, and the results of 2021 are generally higher than those of the same period in 2020. NO₂ and HCHO reached the maximum daily average VCDs on Friday and Thursday, respectively. The weekly variation during the lockdown periods is more subdued compared to the normal days. Due to the decrease in weekend traffic flow, NO₂ has a more significant weekend effect compared to the other two gases.

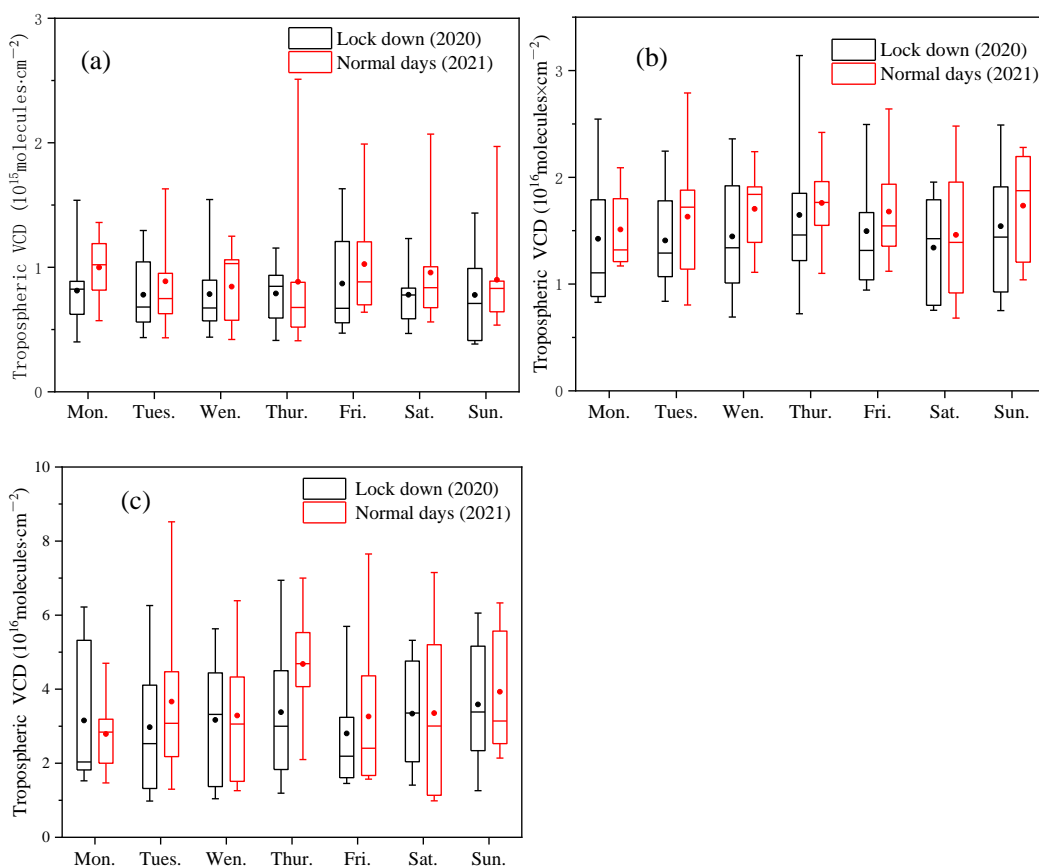


Figure 5. Weekly cycles of (a) NO₂, (b) HCHO and (c) SO₂ VCDs observed over Huaibei during the lockdown period and normal days.

Atmospheric trace gas levels in urban areas are closely related to anthropogenic emissions. The differences between the diurnal variation curves may be caused by the complex interplay between emissions, chemistry and transport. Diurnal variations are critical for understanding the atmospheric chemistry of trace gas species. Figure 6 shows the diurnal variations of the trace gases during the normal days compared to the lockdown period. The diurnal cycle for NO₂, HCHO and SO₂ remained essentially the same during the lockdown period compared to during normal days. NO₂ showed a slight decrease in concentration from morning to noon and then increased in the afternoon. Both HCHO and SO₂ showed an overall trend of first decreasing and then increasing. The HCHO remained at a high concentration until 11:00 am, dropped sharply from 11:00 to 14:00, and then rose in the afternoon. SO₂ had a similar diurnal variation trend compared to HCHO, but it decreased significantly from 8:00 to 9:00 in the morning. During the lockdown period, the

diurnal trend remained the same, but the overall concentrations were lower than those on normal days.

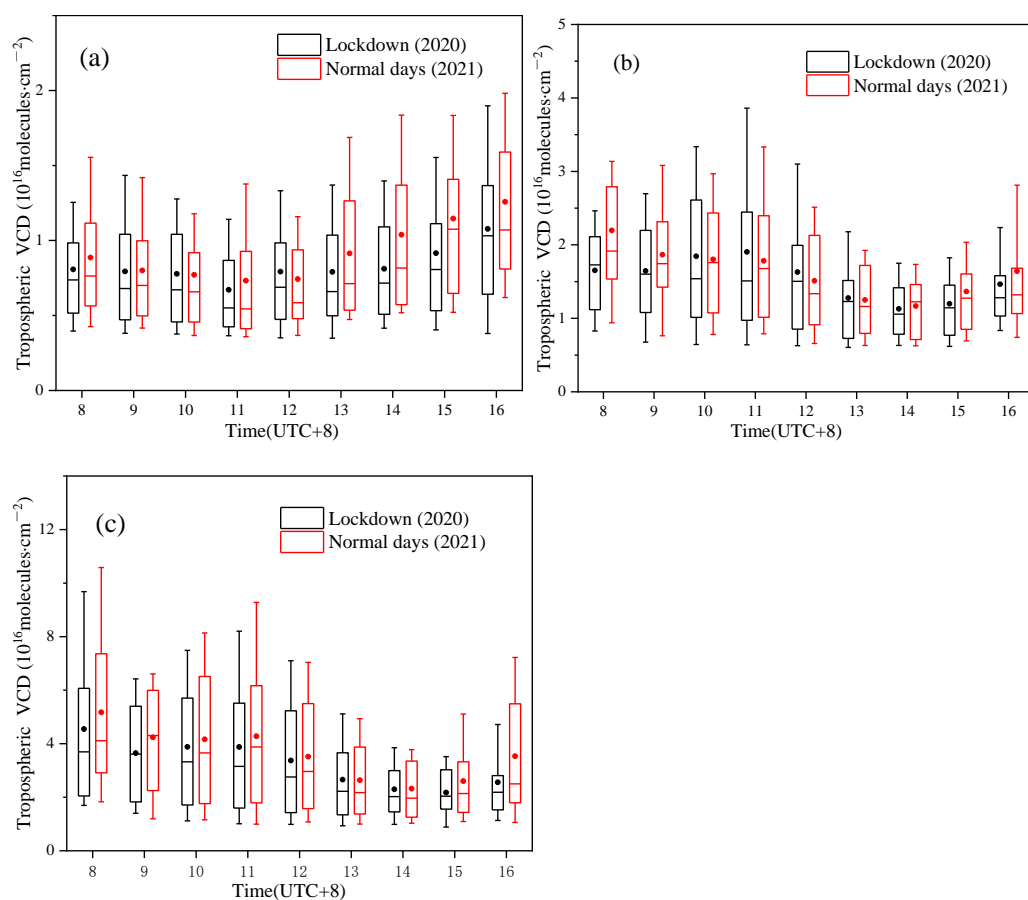


Figure 6. Averaged diurnal variations of (a) NO_2 , (b) HCHO and (c) SO_2 VCDs observed over Huaibei during the lockdown period and normal days.

3.3. Wind Dependence of the Pollutants

The MAX-DOAS station is located in the Northern suburb of Huaibei. Several plastics factories, building material factories, and chemical plants operate in the east and south-west industrial areas. There is an elevated source in the south-east region of the observation station, which has a larger vehicle flux. The industrial activities and vehicle operations lead to significant emissions of NO_2 , HCHO and SO_2 . In the urban center, traffic and anthropogenic emission sources lead to large concentrations of NO_2 and VOCs. In addition, an industrial area located 10 km north of the city potentially contributes to the observed pollutants, depending on meteorological conditions. Figure 7 shows the relationship between the NO_2 , HCHO and SO_2 VCDs and the wind direction and speed from 24 January to 31 March, 2020 and 2021. The trace gas VCDs and wind field data were derived from MAX-DOAS and reanalysis data, respectively. The MAX-DOAS data were averaged hourly for comparison. It can be seen that in 2020 the wind rose (Figure 7) was much more evenly distributed, with easterly and westerly being the most dominant wind directions. In 2021, northerly winds were most frequent. The results show that high NO_2 values were observed in the north-east wind zone in 2021. This could be due to the fact that a large amount of NO_2 was produced by the Eastern elevated source and transported over urban areas by the north-east wind. In 2020, high HCHO and SO_2 values were observed in the same wind zone, potentially due to the transport of pollutants from industrial areas in the north and south-west of the city to the urban area. Higher HCHO and SO_2 values were observed in 2021, potentially caused by urban emissions and atmospheric photochemical reactions.

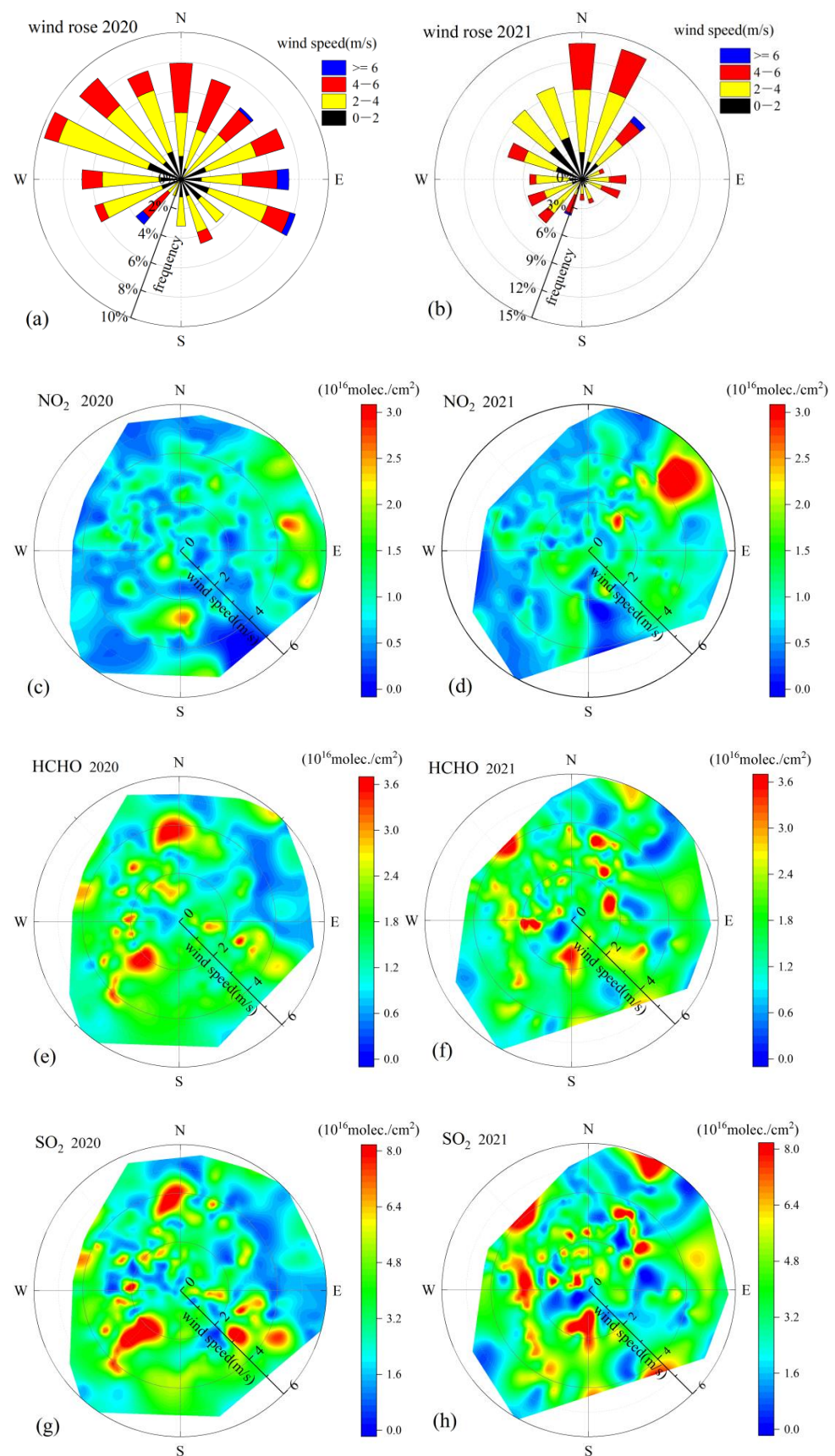


Figure 7. Wind roses in (a) 2020 and (b) 2021. Dependence of (c,d) NO₂, (e,f) HCHO and (g,h) SO₂ VCDs on wind directions and wind speeds in 2020 and 2021.

3.4. In Situ Measurements

Time-series data of in situ instrumental measurements of NO₂, SO₂, PM_{2.5} and O₃ concentrations for 2020 and 2021 are given in Figure 8. SO₂ data will be missing after 15 March 2021. The average concentrations of NO₂, SO₂, PM_{2.5} and O₃ in phase 1 during lockdown in 2020 were 15, 7, 69 and 67 µg/m³, respectively. Compared with 2020, the average concentrations of NO₂ and SO₂ in phase 1 in 2021 increased by 59 and 11%, respectively, and PM_{2.5} and O₃ decreased by 15 and 17%, respectively. In 2021, the near-surface concentrations of NO₂ and SO₂ increased due to traffic and industrial emissions. The decrease in PM_{2.5} and O₃ may be related to primary aerosol emissions and atmospheric photochemical reactions.

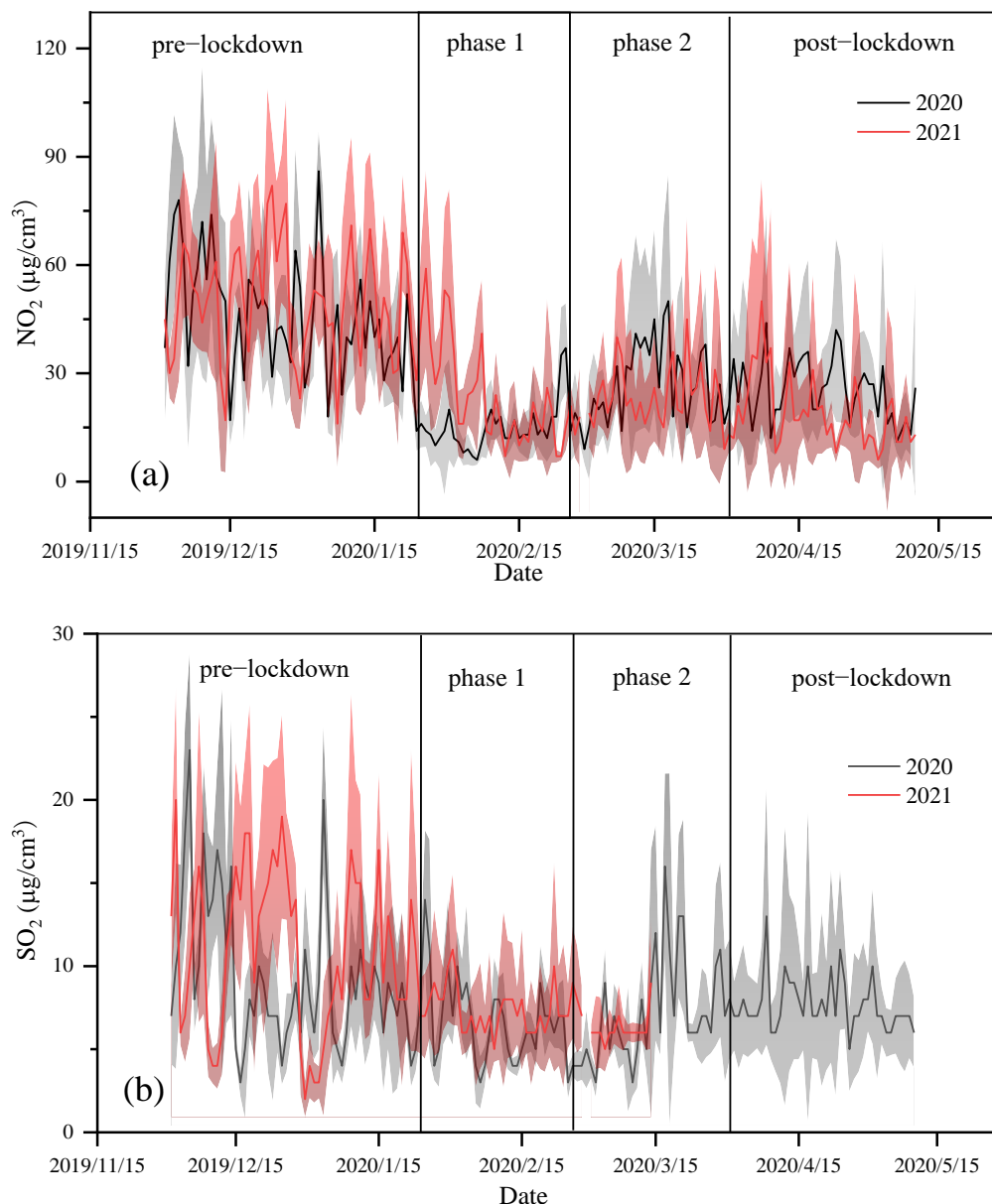


Figure 8. Cont.

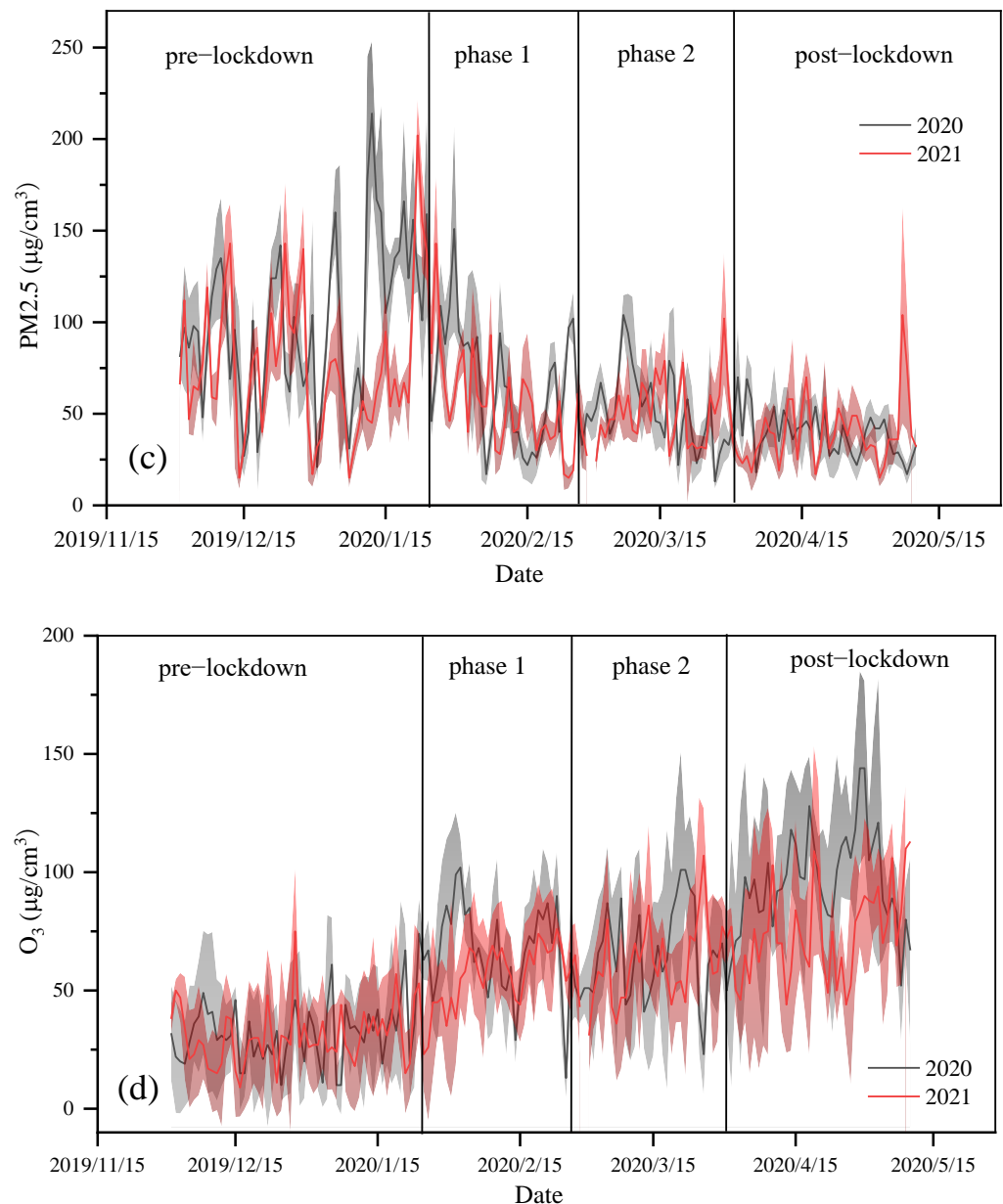


Figure 8. Time series diagram of (a) NO₂, (b) SO₂, (c) PM_{2.5} and (d) O₃ concentrations obtained by using in situ instruments (the shaded area represents the standard deviation of the daily averaged values of different gases).

3.5. HCHO/NO₂ and Source of HCHO

O₃ is widely involved in atmospheric photochemical reactions, and the concentration of near-surface O₃ has become the focus of urban atmospheric environment research. Precursors, such as nitrogen oxides (NO_x), and VOCs emitted by industrial activities, generate O₃ through complex photochemical reactions under ultraviolet radiation. A variety of other hydrocarbons determine the concentration of HCHO. Thus, HCHO is used as an indicator of VOCs. The ratio of HCHO to NO₂ is used to study the influence of NO_x and VOCs on the formation of O₃. Ratios less than 1 and greater than 2 indicate that O₃ production is limited by VOCs and NO_x, respectively, while ratios between 1 and 2 indicate that O₃ is simultaneously affected by both gases. Different from the results reported by Nanjing and Shanghai [12,13], O₃ generation during the winter (gray area) in Huaibei is mainly influenced by NO_x, and O₃ generation in March is influenced by both NO_x and VOCs (Figure 9).

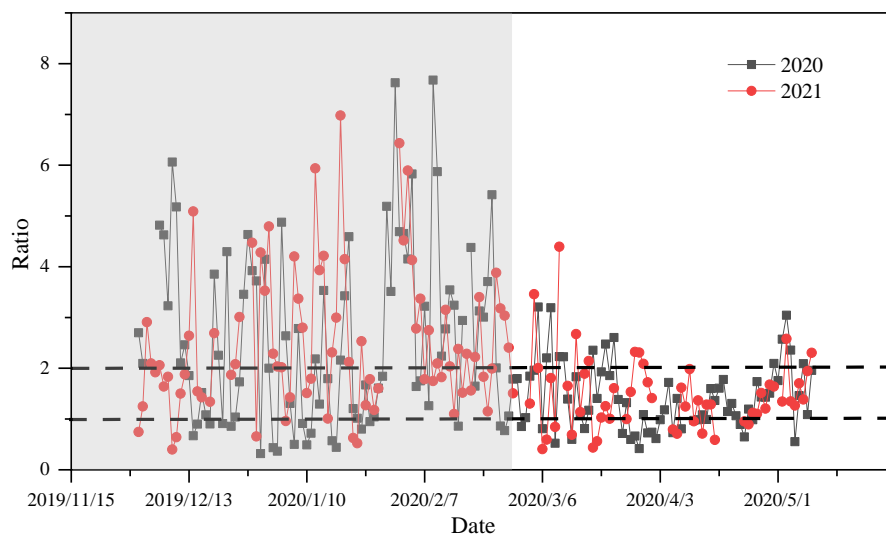


Figure 9. Daily average HCHO/NO₂ ratio at Huaibei in 2020 and 2021.

Determining the sources of pollution is crucial for monitoring air pollution. O₃ is mainly produced through atmospheric photochemical reactions, so O₃ concentrations can be used as an indicator of atmospheric photochemical reaction intensity. Research has shown that HCHO is mainly generated from atmospheric photochemical reactions in the Huairou area of Beijing [10]. To further determine whether the pollution sources of HCHO in Huaibei were due to primary or secondary formations from other VOCs, the correlation of HCHO with primary pollutants (NO₂ and SO₂) or secondary pollutants (O₃) was analyzed (Figure 10). The daily averaged values of different gases for all the observation periods in 2020 and 2021 were selected for the study period. It can be seen from Figure 10 that the correlation coefficients R² of HCHO and SO₂ in 2020 and 2021 are 0.86 and 0.89, respectively. In contrast, the correlation coefficient between NO₂ and HCHO is less than 0.1, and between O₃ and HCHO is less than 0.3. Therefore, HCHO in Huaibei mainly comes from primary industrial emissions related to SO₂, and the proportion of HCHO generated by atmospheric photochemical reactions is low. Temperature changes in spring can affect the natural source emissions of HCHO. Figure 11 shows the temperature changes during the observation periods of the two years. It can be seen that the temperature in the spring did not significantly change in two years. The influence of natural sources on the differences in HCHO concentrations was therefore excluded. In addition, during the cold period in 2021, more heating was needed, probably also contributing to changes in NO₂ and SO₂.

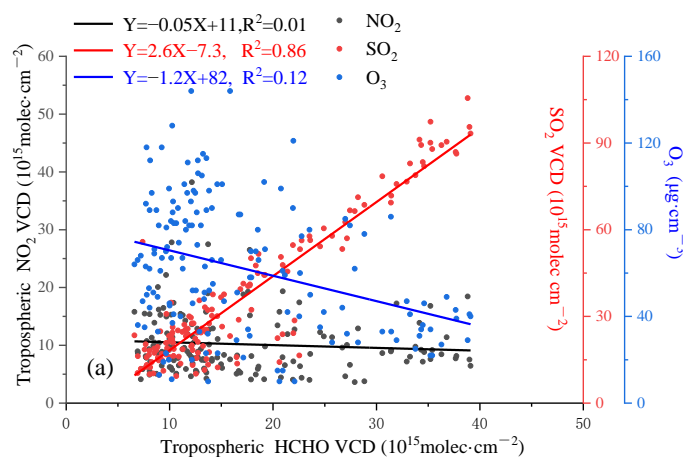


Figure 10. Cont.

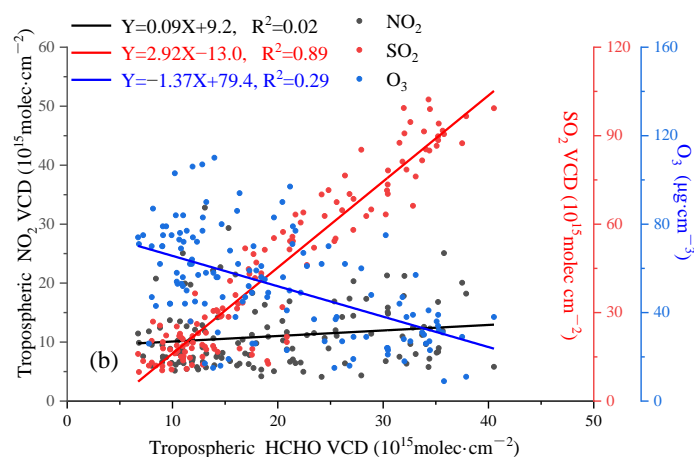


Figure 10. Scatter plots and linear regressions of daily average HCHO VCD measured by MAX-DOAS against NO_2 , SO_2 VCD measured by MAX-DOAS and O_3 measured by an in situ instrument in (a) 2020 and (b) 2021.

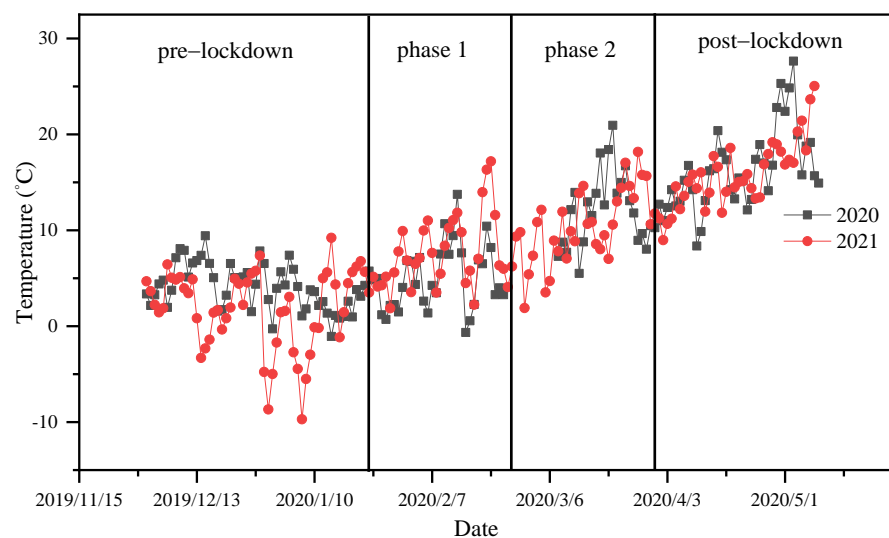


Figure 11. The variation of temperature ($^{\circ}\text{C}$) from the weather station at Huaibei in 2020 and 2021.

4. Discussion

Ground-based MAX-DOAS observations showed that the seasonal and monthly variation characteristics in Huaibei remained unchanged in 2020 and 2021. The concentration of trace gases in winter was significantly higher than in spring, and the monthly mean values of HCHO and SO_2 decreased from December to April of the following year. During the observation period in December 2021, NO_2 , HCHO and SO_2 had the highest monthly mean values, which were 1.57 , 2.82 and 6.69×10^{16} molecules/ cm^2 , respectively. Compared with 2020, the NO_2 concentration increased by 41% during the second stage in 2021, and the changes in HCHO and SO_2 concentrations were not obvious, indicating that the lockdown measures during the epidemic significantly impacted NO_2 emissions.

The weekly circle and diurnal variation results of the pollutant column densities from 24 January to 31 March were analyzed. The weekly circle results showed that the results in 2021 were generally higher than those in 2020, with NO_2 reaching a weekly maximum on Fridays and both HCHO and SO_2 reaching a weekly maximum on Thursdays. NO_2 , HCHO and SO_2 did not show a significant weekend effect. The diurnal variation results show that the results in 2021 are higher than those in 2020 and show obvious diurnal variation characteristics. Among the trace gases, NO_2 had a slight decrease from morning to noon and increased in the afternoon due to the combined effects of light intensity reduction and

emissions. HCHO remained at a high concentration until 11:00 am, decreased sharply from 11:00 to 14:00, and then increased in the afternoon. The trend of SO₂ was similar to that of HCHO, but it drastically decreased from 8:00 to 9:00 in the morning. High values of HCHO and SO₂ were observed in the morning, indicating the existence of nighttime factory emissions.

The wind rose diagrams indicate that the northerly wind prevailed during the lockdown period. The relationship between the pollutant concentration and wind speed and direction was analyzed. The results show that a large amount of NO₂ was emitted by elevated sources in the Eastern part of the city and transported to the urban area by the north-east wind. The high HCHO and SO₂ values in 2020 were mainly caused by emissions from the industrial zone to the north and south-west of the city. The increase in the number of high-value HCHO and SO₂ points in 2021 was mainly caused by an increase in urban emission sources during normal periods. Both HCHO and SO₂ had high values under the same wind field in 2020 and 2021.

The results of the HCHO/NO₂ ratio show that the O₃ content in the Huaibei area is mainly affected by NO_x in winter and jointly affected by NO_x and VOCs in spring. The high correlation between HCHO and SO₂ shows that the HCHO concentration in Huaibei is mainly affected by primary industrial emissions related to SO₂; however, the contribution of atmospheric photochemical reactions to HCHO generation is unclear.

5. Conclusions

We studied the tropospheric NO₂, HCHO and SO₂ VCDs in the Huaibei region based on ground-based MAX-DOAS observations from December 2019 to May 2020 and from December 2020 to May 2021. Anthropogenic activities were reduced during the lockdown period in 2020. The variation in pollution patterns and the impact of lockdown measures on pollutant emissions during the epidemic were analyzed. Compared to the lockdown phase 1 period in 2020, NO₂ emissions increased by 41% in 2021 as the lockdown measures were lifted, while a smaller increase was observed for HCHO and SO₂ (14 and 14%, respectively). The results show that after the city lockdown measures were implemented in Huaibei in 2020, traffic emissions decreased but local industrial production did not significantly change. The observed ratio of HCHO to NO₂ showed that tropospheric ozone production was predominantly NO_x-limited in winter. However, further investigations should be carried out in combination with the vertical distribution of pollutants and compared with satellite data.

Supplementary Materials: The following supporting information can be downloaded at: <https://www.mdpi.com/article/10.3390/atmos14040739/s1>, Figure S1: daily average results of NO₂ from OMI satellites in different time periods; Table S1: different filters and corresponding thresholds applied to the retrieved SCDs; Table S2: the average concentration changes of three gases in four time periods in 2021 compared with the same period in 2020; Figure S2: the RMS results of measured spectra during the entire observation period; Figure S3: the result of the (a) 15° and (b) 30° angles in the same measurement cycle for NO₂ gas in Figure 2 in the main manuscript.

Author Contributions: Conceptualization, F.M., Y.S. and S.L.; methodology, J.L., Q.Z. and F.M.; software, C.Z. and F.M.; validation, Y.S., S.W. and F.Y.; formal analysis, F.M. and F.Y.; investigation, F.M.; resources, Y.S. and S.W.; data curation, Q.Z. and F.Y.; writing—original draft preparation, F.M. and S.L.; writing—review and editing, Q.Z. and J.L.; visualization, C.Z.; supervision, J.L.; project administration, S.L.; funding acquisition, S.L. All authors have read and agreed to the published version of the manuscript.

Funding: This research was funded by the National Natural Science Foundation of China (41875040), the Natural Science Foundation of Anhui Province (2208085QF215), the Youth Innovation Promotion Association, CAS (2019434).

Institutional Review Board Statement: Not applicable.

Informed Consent Statement: Not applicable.

Data Availability Statement: The data presented in this study are available on request from the corresponding author.

Acknowledgments: We thank the Copernicus Atmosphere Monitoring Service (CAMS) for the reanalysis meteorological products and and QDOAS spectral analysis software, respectively. We also thank the China Meteorological Data Service Centre (CMDC) for near-surface meteorological data.

Conflicts of Interest: The authors declare no conflict of interest.

References

1. Vlemmix, T.; Hendrick, F.; Pinardi, G.; De Smedt, I.; Fayt, C.; Hermans, C.; PETERS, A.; Wang, P.; Levelt, P.; Van Roozendaal, M. MAX-DOAS observations of aerosols, formaldehyde and nitrogen dioxide in the Beijing area: Comparison of two profile retrieval approaches. *Atmos. Meas. Tech.* **2015**, *8*, 941–963. [[CrossRef](#)]
2. Tian, X.; Xie, P.; Xu, J.; Li, A.; Wang, Y.; Qin, M.; Hu, Z. Long-term observations of tropospheric NO₂, SO₂ and HCHO by MAX-DOAS in Yangtze River Delta area, China. *J. Environ. Sci.* **2018**, *71*, 207–221. [[CrossRef](#)] [[PubMed](#)]
3. Wang, Y.; Pukite, J.; Wagner, T.; Donner, S.; Beirle, S.; Hilboll, A.; Vrekoussis, M.; Richter, A.; Apituley, A.; PETERS, A.; et al. Vertical Profiles of Tropospheric Ozone From MAX-DOAS Measurements During the CINDI-2 Campaign: Part 1—Development of a New Retrieval Algorithm. *J. Geophys. Res. Atmos.* **2018**, *123*, 10–637. [[CrossRef](#)]
4. Chen, W.T.; Shao, M.; Lu, S.H.; Wang, M.; Zeng, L.M.; Yuan, B.; Liu, Y. Understanding primary and secondary sources of ambient carbonyl compounds in Beijing using the PMF model. *Atmos. Chem. Phys.* **2014**, *14*, 3047–3062. [[CrossRef](#)]
5. Guo, Y.; Li, S.; Mou, F.; Qi, H.; Zhang, Q. Research of NO₂ vertical profiles with look-up table method based on MAX-DOAS. *Chin. Phys. B* **2022**, *31*, 014212. [[CrossRef](#)]
6. Mo, J.; Gong, S.; He, J.; Zhang, L.; Ke, H.; An, X. Quantification of SO₂ Emission Variations and the Corresponding Prediction Improvements Made by Assimilating Ground-Based Observations. *Atmosphere* **2022**, *13*, 470. [[CrossRef](#)]
7. Mak, H.W.L.; Ng, D.C.Y. Spatial and socio-classification of traffic pollutant emissions and associated mortality rates in high-density Hong Kong via improved data analytic approaches. *Int. J. Environ. Res. Public Health* **2021**, *18*, 6532. [[CrossRef](#)]
8. Wei, J.; Li, Z.; Wang, J.; Li, C.; Gupta, P.; Cribb, M. Ground-level gaseous pollutants (NO₂, SO₂, and CO) in China: Daily seamless mapping and spatiotemporal variations. *Atmos. Chem. Phys.* **2023**, *23*, 1511–1532. [[CrossRef](#)]
9. Chan, K.L.; Hartl, A.; Lam, Y.F.; Xie, P.H.; Liu, W.Q.; Cheung, H.M.; Lampel, J.; Pöhler, D.; Li, A.; Xu, J.; et al. Observations of tropospheric NO₂ using ground based MAX-DOAS and OMI measurements during the Shanghai World Expo 2010. *Atmos. Environ.* **2015**, *119*, 45–58. [[CrossRef](#)]
10. Tian, X.; Xie, P.; Xu, J.; Wang, Y.; Li, A.; Wu, F.; Hu, Z.; Liu, C.; Zhang, Q. Ground-based MAX-DOAS observations of tropospheric formaldehyde VCDs and comparisons with the CAMS model at a rural site near Beijing during APEC. *Atmos. Chem. Phys.* **2014**, *19*, 3375–3393. [[CrossRef](#)]
11. Ni, Z.-Z.; Luo, K.; Gao, Y.; Gao, X.; Jiang, F.; Huang, C.; Fan, J.-R.; Fu, J.S.; Chen, C.-H. Spatial–temporal variations and process analysis of O₃ pollution in Hangzhou during the G20 summit. *Atmos. Chem. Phys.* **2020**, *20*, 5963–5976. [[CrossRef](#)]
12. Javed, Z.; Wang, Y.; Xie, M.; Tanvir, A.; Rehman, A.; Ji, X.; Xing, C.; Shakoor, A.; Liu, C. Investigating the Impacts of the COVID-19 Lockdown on Trace Gases Using Ground-Based MAX-DOAS Observations in Nanjing, China. *Remote Sens.* **2020**, *12*, 3939. [[CrossRef](#)]
13. Tanvir, A.; Javed, Z.; Jian, Z.; Zhang, S.; Bilal, M.; Xue, R.; Wang, S.; Bin, Z. Ground-Based MAX-DOAS Observations of Tropospheric NO₂ and HCHO During COVID-19 Lockdown and Spring Festival Over Shanghai, China. *Remote Sens.* **2021**, *13*, 488. [[CrossRef](#)]
14. Muhammad, S.; Long, X.; Salman, M. COVID-19 pandemic and environmental pollution: A blessing in disguise? *Sci. Total Environ.* **2020**, *728*, 138820. [[CrossRef](#)] [[PubMed](#)]
15. Sharma, S.; Zhang, M.; Anshika; Gao, J.; Zhang, H.; Kota, S.H. Effect of restricted emissions during COVID-19 on air quality in India. *Sci. Total Environ.* **2020**, *728*, 138878. [[CrossRef](#)] [[PubMed](#)]
16. Roşu, A.; Constantin, D.-E.; Voiculescu, M.; Arseni, M.; Roşu, B.; Merlaud, A.; Van Roozendaal, M.; Georgescu, P.L. Assessment of NO₂ Pollution Level during the COVID-19 Lockdown in a Romanian City. *Int. J. Environ. Res. Public Health* **2021**, *18*, 544. [[CrossRef](#)]
17. Choi, Y.; Kanaya, Y.; Takashima, H.; Park, K.; Lee, H.; Chong, J.; Kim, J.H.; Park, J.-S. Changes in tropospheric nitrogen dioxide vertical column densities over Japan and Korea during the COVID-19 using Pandora and MAX-DOAS. *Aerosol Air Qual. Res.* **2021**, *23*, 220145. [[CrossRef](#)]
18. Fan, C.; Li, Y.; Guang, J.; Li, Z.; Elnashar, A.; Allam, M.; De Leeuw, G. The Impact of the Control Measures during the COVID-19 Outbreak on Air Pollution in China. *Remote Sens.* **2020**, *12*, 1613. [[CrossRef](#)]
19. Mahato, S.; Pal, S.; Ghosh, K.G. Effect of lockdown amid COVID-19 pandemic on air quality of the megacity Delhi, India. *Sci. Total Environ.* **2020**, *730*, 139086. [[CrossRef](#)]
20. Mou, F.; Luo, J.; Li, S.; Shan, W.; Hu, L. Vertical profile of aerosol extinction based on the measurement of O₄ of multi-elevation angles with MAX-DOAS. *Chin. Phys. B* **2019**, *28*, 084212. [[CrossRef](#)]
21. Zhang, Q.; Mou, F.; Li, S.; Li, A.; Wang, X.; Sun, Y. Quantifying emission fluxes of atmospheric pollutants from mobile differential optical absorption spectroscopic (DOAS) observations. *Spectrochim. Acta A* **2023**, *286*, 121959. [[CrossRef](#)] [[PubMed](#)]

22. Xu, S.; Wang, S.; Xia, M.; Lin, H.; Xing, C.; Ji, X.; Su, W.; Tan, W.; Liu, C.; Hu, Q. Observations by Ground-Based MAX-DOAS of the Vertical Characters of Winter Pollution and the Influencing Factors of HONO Generation in Shanghai, China. *Remote Sens.* **2021**, *13*, 3518. [[CrossRef](#)]
23. Mak, H.W.L.; Laughner, J.L.; Fung, J.C.H.; Zhu, Q.; Cohen, R.C. Improved Satellite Retrieval of Tropospheric NO₂ Column Density via Updating of Air Mass Factor (AMF): Case Study of Southern China. *Remote Sens.* **2018**, *10*, 1789. [[CrossRef](#)]
24. Javed, Z.; Liu, C.; Ullah, K.; Tan, W.; Xing, C.; Liu, H. Investigating the Effect of Different Meteorological Conditions on MAX-DOAS Observations of NO₂ and CHOCHO in Hefei, China. *Atmosphere* **2019**, *10*, 353. [[CrossRef](#)]
25. Javed, Z.; Liu, C.; Khokhar, M.F.; Xing, C.; Tan, W.; Subhani, M.A.; Rehman, A.; Tanvir, A. Investigating the impact of Glyoxal retrieval from MAX-DOAS observations during haze and non-haze conditions in Beijing. *J. Environ. Sci.* **2019**, *80*, 296–305. [[CrossRef](#)]
26. Danckaert, T.; Van Roozendaal, M.; Letocart, V.; Merlaud, A.; Pinaridi, G. *QDOAS Software User Manual*; Belgian Institute for Space Aeronomy: Brussels, Belgium, 2017.
27. Platt, U.; Stutz, J. *Differential Optical Absorption Spectroscopy—Principles and Applications*; Springer: Berlin/Heidelberg, Germany, 2008.
28. Vandaele, A.C.; Hermans, C.; Simon, P.C.; Carleer, M.; Colin, R.; Fally, S.; Mérienne, M.F.; Jenouvrier, A.; Coquart, B. Measurements of the NO₂ absorption cross-section from 42,000 cm⁻¹ to 10,000 cm⁻¹ (238–1000 nm) at 220 K and 294 K. *J. Quant. Spectrosc. Radiat. Transf.* **1998**, *59*, 171–184. [[CrossRef](#)]
29. Serdyuchenko, A.; Gorshchev, V.; Weber, M.; Chehade, W.; Burrows, J.P. High spectral resolution ozone absorption cross-sections—Part 2: Temperature dependence. *Atmos. Meas. Tech.* **2014**, *7*, 625–636. [[CrossRef](#)]
30. Thalman, R.; Volkamer, R. Temperature dependent absorption cross-sections of O₂–O₂ collision pairs between 340 and 630 nm and at atmospherically relevant pressure. *Phys. Chem. Chem. Phys.* **2013**, *15*, 15371–15381. [[CrossRef](#)] [[PubMed](#)]
31. Meller, R.; Moortgat, G.K. Temperature dependence of the absorption cross sections of formaldehyde between 223 and 323 K in the wavelength range 225–375 nm. *J. Geophys. Res. Space Phys.* **2000**, *105*, 7089–7101. [[CrossRef](#)]
32. Fleischmann, O.C.; Hartmann, M.; Burrows, J.P.; Orphal, J. New ultraviolet absorption cross-sections of BrO at atmospheric temperatures measured by time-windowing Fourier transform spectroscopy. *J. Photochem. Photobiol. A Chem.* **2004**, *168*, 117–132. [[CrossRef](#)]
33. Zhang, Q.; Mou, F.; Wei, S.; Luo, J.; Wang, X.; Li, S. Vertical profiles of aerosol and NO₂ based on mobile multi-axis differential absorption spectroscopy. *Atmos. Pollut. Res.* **2023**, *2023*, 101732. [[CrossRef](#)]
34. Wang, Y.; Li, A.; Xie, P.H.; Chen, H.; Mou, F.S.; Xu, J.; Wu, F.-C.; Zeng, Y.; Liu, J.-G.; Liu, W.-Q. Measuring tropospheric vertical distribution and vertical column density of NO₂ by multi-axis differential optical absorption spectroscopy. *Acta Phys. Sin.* **2013**, *16*, 200705. [[CrossRef](#)]
35. Wang, Y.; Lampel, J.; Xie, P.; Beirle, S.; Li, A.; Wu, D.; Wagner, T. Ground-based MAX-DOAS observations of tropospheric aerosols, NO₂, SO₂ and HCHO in Wuxi, China, from 2011 to 2014. *Atmos. Chem. Phys.* **2017**, *17*, 2189–2215. [[CrossRef](#)]

Disclaimer/Publisher’s Note: The statements, opinions and data contained in all publications are solely those of the individual author(s) and contributor(s) and not of MDPI and/or the editor(s). MDPI and/or the editor(s) disclaim responsibility for any injury to people or property resulting from any ideas, methods, instructions or products referred to in the content.